
Effective Learning of a GMRF Mixture Model

Shahaf E. Finder¹ · Eran Treister¹ · Oren Freifeld¹

Received: date / Accepted: date

Abstract Learning a Gaussian Mixture Model (GMM) is hard when the number of parameters is too large given the amount of available data. As a remedy, we propose restricting the GMM to a Gaussian Markov Random Field Mixture Model (GMRF-MM), as well as a new method for estimating the latter’s sparse precision (*i.e.*, inverse covariance) matrices. When the sparsity pattern of each matrix is known, we propose an efficient optimization method for the Maximum Likelihood Estimate (MLE) of that matrix. When it is unknown, we utilize the popular Graphical LASSO (GLASSO) to estimate that pattern. However, we show that even for a single Gaussian, when GLASSO is tuned to successfully estimate the sparsity pattern, it does so at the price of a substantial bias of the values of the nonzero entries of the matrix, and we show that this problem only worsens in a mixture setting. To overcome this, we discard the non-zero values estimated by GLASSO, keep only its pattern estimate and use it within the proposed MLE method. This yields an effective two-step procedure that removes the bias. We show that our “debiasing” approach outperforms GLASSO in both the single-GMRF and the GMRF-MM cases. We also show that when learning priors for image patches, our method outperforms GLASSO even if we merely use an educated guess about the sparsity pattern, and that our GMRF-MM outperforms the baseline GMM on real and synthetic high-dimensional datasets. Our code is available at <https://github.com/shahaffind/GMRF-MM>.

Keywords GMM · Gaussian Markov Random Field · Graphical LASSO · Over-parameterization

1 Introduction

The ubiquitous Gaussian Mixture Model (GMM) (*e.g.*, see [Hastie et al. \(2005\)](#)) is widely used for modeling complex non-unimodal distributions, and has found applications in nu-

This research was partially supported by the Israeli Council for Higher Education (CHE) via Data Science Research Center, Ben-Gurion University of the Negev, Israel.

Shahaf E. Finder
E-mail: finders@post.bgu.ac.il

¹ Department of Computer Science, Ben-Gurion University, Israel

merous fields including, but not limited to, computer vision and image processing (Jepson and Black, 1993; Zhuang et al., 1996; Stauffer and Grimson, 1999; Chen et al., 2004; Zoran and Weiss, 2011; Freifeld et al., 2015; Pappas and Elad, 2015; Niknejad et al., 2019), signal processing (Vo and Ma, 2006; Vila and Schniter, 2013), speech recognition (Reynolds and Rose, 1995; Reynolds et al., 2000), anomaly detection (Basharat et al., 2008; Idé et al., 2016) and biology (Kawabata, 2008; Nagoshi et al., 2004). The number of parameters in each Gaussian, however, is quadratic in n , the dimension of the data, and thus, when there is not enough data to support an effective estimation, the GMM is prone to become over-parameterized (Bouveyron et al., 2007; McLachlan et al., 2019), hindering the applicability of the model. Moreover, in certain settings (though not always), K , the number of Gaussians in the mixture, also tends to grow with n , making the over-parameterization problem worse since the average number of points per Gaussian decreases when K increases. For example, Zoran and Weiss (2011), who learned a GMM over 8-by-8 image patches (*i.e.*, $n = 64$), reported that K needed to be as high as 200 to produce good results. Other scenarios (*e.g.*, larger image patches) might require even a higher K .

To overcome the over-parameterization problem, we propose reducing the number of parameters by restricting each of the components of the GMM to be a Gaussian Markov Random Field (GMRF), thereby obtaining a GMRF Mixture Model (GMRF-MM). A GMRF is a Gaussian whose precision matrix (namely, inverse covariance), denoted by \mathbf{Q} , is sparse. Such a \mathbf{Q} is associated with a probabilistic graphical model (Koller and Friedman, 2009; Rue and Held, 2005); see § 2.

Remark 1 The GMRF-MM should not be confused with models that combine a (typically low-dimensional) GMM with a discrete-state Markov Random Field (MRF) over the spatially- (or temporally-) dependent labels associated with the observations (as was done in, *e.g.*, Pyun et al. (2007); Uziel et al. (2019)).

The GMRF assumption, common in the single-Gaussian case (see Rue and Held (2005); Grenander and Miller (2007) and references therein), is rarely used in the case of mixtures. This raises a natural question: how come the idea of reducing the number of parameters by restricting the GMM to a GMRF-MM has been hardly explored so far? We suspect that a plausible explanation for this is that traditional methods for estimating the sparse \mathbf{Q} (in the single-Gaussian case, which is an indispensable building block in the mixture setting) are not effective enough, especially when the sparsity pattern (*i.e.*, the locations of the zero entries of \mathbf{Q}) is unknown. For example, consider the widely-used Graphical LASSO (GLASSO, Friedman et al. (2008)), which is based on an ℓ_1 penalty (see also Hsieh et al. (2013, 2014); Treister et al. (2016); Bollhöfer et al. (2019); Wang and Jiang (2020), and other related solvers based on ℓ_1 that approximate GLASSO Oh et al. (2014); Jelisavcic et al. (2018); Khare et al. (2019)). In this paper we show that even when GLASSO’s regularization parameter is tuned to successfully estimate the sparsity pattern, GLASSO substantially biases the values of the nonzero entries of \mathbf{Q} . In fact, we show this undesirable effect is present regardless whether one excludes the diagonal terms in \mathbf{Q} from the ℓ_1 penalty (Wainwright, 2019) or not. Importantly, we show that the negative effect of this bias on the resulting model only worsens in the mixture case, which is the setting this paper focuses on. Thus, the seemingly-natural choice of GMM+GLASSO (Azizyan et al., 2015; Krishnamurthy, 2011; Lotsi and Wit, 2016; Yang et al., 2014; Tavassolipour et al., 2019) might lead to poor estimates, rendering the GMRF-MM impractical. In fact, we show that GMM+GLASSO can obtain worse results than the baseline (*i.e.*, non-regularized) GMM even when data is scarce.

In this work we propose a framework for an effective and efficient learning a GMRF-MM. Whenever possible, and because of the aforementioned bias, it is beneficial to learn a

GMRF-MM using a pre-defined sparsity. Indeed, in many applications the sparsity pattern is either known or can be assumed via an educated guess; *e.g.*, this is the case in many successful computer-vision Markov Random Field models (Li, 1994; Roth and Black, 2005) or in Geoscience where regions in geographical maps are often assumed to exhibit a Markovian structure (Song et al., 2008). In such cases, we propose to estimate the sparse \mathbf{Q} using a Newton-type optimization method for finding the appropriately-constrained Maximum Likelihood Estimate (MLE). When the sparsity pattern itself must be estimated, we employ a two-step procedure. First, we solve the GLASSO problem; this can be done using a variety of available methods mentioned earlier. Next, we *discard the GLASSO estimates* of the nonzero entries \mathbf{Q} because these are usually *substantially biased* and keep only the GLASSO estimate of the sparsity pattern. To find the “debiased” MLE, we use that Newton-type method given the estimated sparsity pattern. This “debiasing” procedure effectively removes the GLASSO bias.

Our experiments show that the proposed method outperforms GLASSO in both the single-Gaussian and the GMRF-MM cases. We also show that when learning a GMM over image patches, the proposed method outperforms GLASSO in both cases: 1) when we merely make an educated guess about the sparsity pattern; 2) when we debias the GLASSO estimates. In addition, we show that, with the proposed method, a GMRF-MM outperforms a baseline GMM on real and synthetic high-dimensional datasets.

To summarize, **our key contributions are as follows.**

1. We propose a framework for learning a GMM that overcomes the over-parameterization problem by assuming each component is a GMRF.
2. When the sparsity pattern, Ω , is known, we propose an efficient optimization method for finding the MLE of \mathbf{Q} . When Ω is unknown, we use 2-step procedure that *debases* (*i.e.*, removes the bias of) the GLASSO estimate.
3. We show that estimating the GMRF-MM with the debiased GLASSO lets us learn an effective GMRF-MM of unknown sparsity patterns (Ω is component-specific).
4. We provide new theoretical results that further explain the GLASSO bias (with either a penalized or non-penalized diagonal).

2 Preliminaries

A K -component GMM in \mathbb{R}^n is given by the following probability density function (pdf):

$$p(\mathbf{x}; \Theta) = \sum_{k=1}^K \pi_k \mathcal{N}(\mathbf{x}; \boldsymbol{\mu}_k, \boldsymbol{\Sigma}_k) \quad \mathbf{x} \in \mathbb{R}^n \quad (1)$$

where $\Theta = \{\boldsymbol{\mu}_k, \boldsymbol{\Sigma}_k, \pi_k\}_{k=1}^K$, $\boldsymbol{\mu}_k \in \mathbb{R}^n$ and $\boldsymbol{\Sigma}_k \in \mathbb{R}^{n \times n}$ are the mean and (symmetric positive-definite) covariance matrix of Gaussian k , the weights $(\pi_k)_{k=1}^K$ form a convex combination, and

$$\mathcal{N}(\mathbf{x}; \boldsymbol{\mu}, \boldsymbol{\Sigma}) \triangleq \frac{1}{(2\pi)^{n/2} |\boldsymbol{\Sigma}|^{1/2}} \exp\left(-\frac{1}{2} \|\mathbf{x} - \boldsymbol{\mu}\|_{\boldsymbol{\Sigma}^{-1}}^2\right) \quad (2)$$

where

$$\|\mathbf{x} - \boldsymbol{\mu}\|_{\boldsymbol{\Sigma}^{-1}}^2 \triangleq (\mathbf{x} - \boldsymbol{\mu})^T \boldsymbol{\Sigma}^{-1} (\mathbf{x} - \boldsymbol{\mu}). \quad (3)$$

Given N *i.i.d.* observations, $(\mathbf{x}_i)_{i=1}^N \subset \mathbb{R}^n$, drawn from a GMM parameterized by Θ , the MLE of Θ is

$$\hat{\Theta}_{\text{MLE}} = \arg \max_{\Theta} \prod_{i=1}^N \sum_{k=1}^K \pi_k \mathcal{N}(\mathbf{x}; \boldsymbol{\mu}_k, \boldsymbol{\Sigma}_k). \quad (4)$$

A closed-form solution for Eq. (4) does not exist. Thus, a popular solution is to introduce auxiliary variables (called hard assignments or labels) and to use *an* Expectation-Maximization (EM) algorithm, which works iteratively by alternating between two steps:

1. An **E step** where, for each $i \in \{1, \dots, N\}$ and each $k \in \{1, \dots, K\}$, w_{ki} , the soft assignment of data point \mathbf{x}_i to Gaussian k , is computed;
2. An **M step**, which maximizes, w.r.t. Θ , the conditional expectation of the so-called complete-data log-likelihood given those soft assignments.

For more details see [McLachlan et al. \(2019\)](#). Let $\mathbf{Q}_k = \boldsymbol{\Sigma}_k^{-1}$ denote the precision matrix of Gaussian k . It can be shown that, during the M step, the estimation of $\boldsymbol{\Sigma}_k$, the covariance of Gaussian k , is equivalent to the MLE of the covariance in a single Gaussian while also taking the weights (*i.e.*, the soft assignments) into account. Due to the invariance property of the MLE ([Silvey, 1970](#)), we can also reformulate this in terms of the (weighted) MLE of \mathbf{Q}_k . That is, given the (weighted) empirical covariance matrix

$$\mathbf{S}_k = \frac{1}{\sum_i w_{ki}} \sum_{i=1}^N w_{ki} (\mathbf{x}_i - \hat{\boldsymbol{\mu}}_k)(\mathbf{x}_i - \hat{\boldsymbol{\mu}}_k)^T \quad (5)$$

(where $\hat{\boldsymbol{\mu}}_k$ is the weighted sample mean of Gaussian k), the MLE of \mathbf{Q} is obtained by minimizing the negative log-likelihood (for a single Gaussian, and when discarding constants),

$$\mathcal{L}(\mathbf{Q}_k) = -\log \det \mathbf{Q}_k + \text{tr}(\mathbf{Q}_k \mathbf{S}_k) \quad (6)$$

(where $\text{tr}(\cdot)$ denotes a matrix trace) w.r.t. \mathbf{Q}_k . Importantly, the optimization is done subject to the constraint that $\mathbf{Q}_k \succ 0$ (*i.e.*, \mathbf{Q}_k is SPD). Since the function in Eq. (6) is convex, a global minimum is found by setting the gradient

$$\nabla \mathcal{L}(\mathbf{Q}_k) = \mathbf{S}_k - \mathbf{Q}_k^{-1} \quad (7)$$

to zero, leading to the known result,

$$\hat{\mathbf{Q}}_{\text{MLE}} = \mathbf{S}_k^{-1}. \quad (8)$$

This closed-form estimator, however, is oblivious to possible constraints on, or a regularization over, \mathbf{Q}_k . Particularly, a regularization is necessary when \mathbf{S}_k is rank deficient, in which case the closed-form estimator in Eq. (8) is undefined (since the matrix is not invertible). Such a situation can occur during the EM process, especially when the number of data samples is small.

2.1 GMRF and Graphical LASSO

Let $\mathbf{x} = (x_1, \dots, x_n) \sim \mathcal{N}(\boldsymbol{\mu}, \boldsymbol{\Sigma})$. Define a graph $\mathcal{G} = (V, E)$, whose nodes are $V = \{1, \dots, n\}$ and its (undirected) edges, E , are defined such that $(i, j) \notin E$ if and only if $x_i \perp x_j | x_{-ij}$ where $x_{-ij} = \{x_k | k \notin \{i, j\}\}$. The notation $x_i \perp x_j | x_{-ij}$ indicates that conditioned on the variables in all the *other* nodes, the two variables, x_i and x_j , are conditionally

independent. We then say that \mathbf{x} is a GMRF w.r.t. \mathcal{G} . It can be shown (Rue and Held, 2005) that the precision matrix, $\mathbf{Q} = \boldsymbol{\Sigma}^{-1}$, satisfies

$$x_i \perp x_j | x_{-ij} \iff \mathbf{Q}_{ij} = 0. \quad (9)$$

Thus, assuming that \mathbf{Q} is sparse implies a probabilistic graphical model with a statistical interpretation that can be justified, either exactly or approximately, in many applications. The sparsity of the graph, however, adds a constraint that must be addressed during the process of the estimation of \mathbf{Q} . Particularly, the closed-form solution in Eq. (8) is no longer applicable as it usually violates that constraint. When the sparsity pattern Ω is known, we can use gradient-based optimization methods that constrain the minimizer to Ω ; *i.e.*, such a method would solve

$$\boxed{\arg \min_{\mathbf{Q} \succ \mathbf{0}} \mathcal{L}(\mathbf{Q}) \text{ subject to } \text{Supp}(\mathbf{Q}) \subseteq \Omega} \quad (10)$$

where $\text{Supp}(\mathbf{Q}) = \{(i, j) \mid \mathbf{Q}_{ij} = \mathbf{Q}_{ji} \neq 0\}$, and $\Omega \subseteq (1, \dots, n) \times (1, \dots, n)$ is a known set of possible nonzero entries. We will return to this problem in § 3 where we propose an efficient method to solve it. When Ω is unknown, a popular approach is to use the GLASSO estimator (Friedman et al., 2008):

$$\boxed{\arg \min_{\mathbf{Q} \succ \mathbf{0}} \mathcal{L}(\mathbf{Q}) + \lambda \|\mathbf{Q}\|_1} \quad (11)$$

where $\|\bullet\|_1$ is the element-wise matrix ℓ_1 norm, and $\lambda > 0$ is a regularization parameter. The addition of the ℓ_1 penalty promotes the sparsity of the minimizer, thus implying a graphical model according to Eq. (9), freeing the user from having to know or assume the sparsity pattern. A common variant of (11) does not include the diagonal terms on \mathbf{Q} is the ℓ_1 penalty term (Wainwright, 2019), to reduce the bias of the diagonal terms which are known to be non-zero. As we will show, however, this method has a main drawback.

3 Method

We now show the estimation process of a GMRF-MM. To simplify the notation, in the remainder of this section we drop the subscripted k (*e.g.*, we will write \mathbf{Q} instead of \mathbf{Q}_k). When adding a constraint or a penalty over \mathbf{Q} , usually there is no longer a closed-form solution for the minimizer of Eq. (6) during the M-step. Particularly, this happens in the two cases considered here: the minimization problem in Eq. (10), when the sparsity pattern of \mathbf{Q} is assumed to be known, and in Eq. (11) (*i.e.*, GLASSO), when that pattern is unknown and an ℓ_1 regularization is used to promote sparsity. In both these cases, we handle the minimization via an appropriate gradient-based iterative method. Any such method first computes a search direction that involves the gradient from Eq. (7), and then takes a step in that direction. That is, the update at iteration t is given by

$$\mathbf{Q}^{(t)} = \mathbf{Q}^{(t-1)} + \alpha^{(t)} \boldsymbol{\Delta}^{(t)}, \quad (12)$$

where $\boldsymbol{\Delta}^{(t)}$ is the search direction and $\alpha^{(t)}$ is the step size, usually obtained by a line search. For example, if we use Gradient Descent to solve Eq. (6), we have $\boldsymbol{\Delta}^{(t)} = -\nabla \mathcal{L}(\mathbf{Q}^{(t-1)})$. In order to impose a given sparsity pattern Ω on the solution, it is possible to project the gradient-descent direction to Ω . To solve the GLASSO problem (Eq. (11)) one may use a solver that is based on the proximity operator (known as “soft-thresholding”) to handle the ℓ_1 penalty. Below we describe these approaches in more detail.

3.1 Estimating \mathbf{Q} with a known sparsity pattern

Suppose that we wish to solve Eq. (10). One main problem arises in this case: any gradient-based approach requires the computation of \mathbf{Q}^{-1} at each step. This is expensive since \mathbf{Q}^{-1} is usually a dense matrix even if \mathbf{Q} itself is sparse. Moreover, if we wish to project the gradient to a given sparsity pattern (compute arbitrary entries from the gradient), there is no easy way to compute only the relevant entries of \mathbf{Q}^{-1} without computing all the entries first. An exception of this is when the underlying graph of \mathbf{Q} is assumed to be chordal; see the following remark for details.

Remark 2 When the underlying graph of \mathbf{Q} is assumed to be chordal, it is possible to compute the entries (i, j) of \mathbf{Q}^{-1} where $\mathbf{Q}_{ij} \neq 0$ efficiently (Vandenberghe and Andersen, 2015). Similarly, if the pattern in Ω is chordal, it is possible to solve Eq. (10) by a recursive elimination. In addition, one can extend the allowed nonzero pattern of \mathbf{Q} to be chordal (Zhang et al., 2018), and use the extended pattern to approximate the solution of Eq. (10) for non-chordal graphs. Either way, that is not the approach we follow here, since the graphs that we consider are non-chordal, and while their associated matrices fairly large, they are still small enough to be inverted at a reasonable cost.

When the optimization problem in Eq. (6) is ill-conditioned, first-order methods might require numerous iterations, and each such iteration requires the inversion operation. To avoid the repeated matrix inversions in such problems, it is common to solve the optimization problem by using a second-order approximation for obtaining the Newton descent direction, using the n^2 -by- n^2 Hessian

$$\nabla^2 \mathcal{L}(\mathbf{Q}) = \mathbf{Q}^{-1} \otimes \mathbf{Q}^{-1} \quad (13)$$

where \otimes is the Kronecker product. By definition, the computation of \mathbf{Q}^{-1} from the gradient in Eq. (7) can be reused for the Hessian in Eq. (13) – that is a main advantage of second-order methods. The Newton direction Δ for Eq. (10) is obtained by solving the *projected Newton problem*:

$$\min_{\Delta: \text{Supp}(\Delta) \subseteq \Omega} \text{tr}(\nabla \mathcal{L}(\mathbf{Q}) \Delta) + \frac{1}{2} \text{tr}(\Delta \mathbf{Q}^{-1} \Delta \mathbf{Q}^{-1}). \quad (14)$$

The Hessian matrix (Eq. (13)) might be dense and large, but multiplying it with a sparse descent direction Δ and projecting the result to Ω can be obtained efficiently (Hsieh et al., 2014; Treister and Turek, 2014). Particularly, the Hessian matrix never needs to be explicitly formed or stored. This allows us to efficiently solve Eq. (14) for a given sparsity pattern Ω using an iterative method. The direction can be found by setting the gradient of Eq. (14) to 0, leading to the following equation:

$$\mathbf{Q}^{-1} \Delta \mathbf{Q}^{-1} = -\nabla \mathcal{L}(\mathbf{Q}). \quad (15)$$

To solve it we use the projected and Preconditioned Conjugate Gradient (PCG) method (Saad, 2003), which is relatively insensitive to a high condition number; note that the conditioning of the problem (the eigenvalues of the Hessian Eq. (13)) depends on the estimated matrix \mathbf{Q} itself, and can be arbitrarily high.

Algorithm 1 presents the method for estimating the MLE subject to a given support. The projected Newton problem (Eq. (14)) is solved in the inner loop of the algorithm, where the projected and Preconditioned Conjugate Gradient (projPCG) method is applied iteratively, to solve the linear Newton problem (Eq. (15)) subject to the given support. In this method,

Algorithm 1: Estimating \mathbf{Q} with a known support

Input: $\mathbf{S}, \Omega, \mathbf{Q}^{(0)}$

- 1 **for** $t = 1, 2, \dots$ **do**
- 2 $\hat{\mathbf{G}}^{(t)} \leftarrow \mathbf{S} - (\mathbf{Q}^{(t-1)})^{-1}$
- 3 $\mathbf{G}^{(t)} \leftarrow$ Project $\hat{\mathbf{G}}^{(t)}$ using the support Ω
- 4 $\Delta^{(t)} \leftarrow$ projPCG($\mathbf{Q}^{(t-1)}, \mathbf{G}^{(t)}, \Omega$)
- 5 $\alpha^{(t)} \leftarrow$ Armijo line-search($\mathbf{Q}^{(t-1)}, \mathbf{G}^{(t)}, \Delta^{(t)}$)
- 6 $\mathbf{Q}^{(t)} \leftarrow \mathbf{Q}^{(t-1)} + \alpha^{(t)} \Delta^{(t)}$

Output: $\mathbf{Q}^{(t)}$

each PCG step (which mostly includes the multiplication of the Hessian with the previous direction) is projected to the given support to maintain the desired sparsity pattern. After calculating the descent direction Δ , we perform an Armijo line search to find the optimal step size. The line search also verifies the descent result is an SPD matrix.

The preconditioner M that we use inside projPCG is diagonal; *i.e.*, it has a weight for each entry of Δ_{ij} . We define the weight M_{ij} for the entry (i, j) to be the corresponding diagonal element of the Hessian, if one also take the symmetry of the Δ into account. More explicitly

$$M_{ij} = \begin{cases} \mathbf{Q}_{ii}^{-1} \mathbf{Q}_{jj}^{-1} + (\mathbf{Q}_{ij}^{-1})^2, & i \neq j \\ (\mathbf{Q}_{ii}^{-1})^2, & i = j \end{cases}. \quad (16)$$

3.2 Estimating \mathbf{Q} with an unknown sparsity pattern

If Ω is unknown a-priori, then one of the popular options for finding it is the GLASSO (Eq. (11)). To solve this problem, the proximal Newton method is often used and is obtained by adding the ℓ_1 regularization term $\lambda \|\mathbf{Q} + \Delta\|_1$ to the quadratic objective like in Eq. (14), which becomes a LASSO problem. The LASSO problem is then often restricted to a given support according to an active-set approach (Hsieh et al., 2014; Treister and Turek, 2014), and is solved using Coordinate Descent (Friedman et al., 2010) or the (projected and preconditioned) Conjugate Gradient for the LASSO problem (Zibulevsky and Elad, 2010; Treister and Yavneh, 2012). Once the LASSO problem is solved, a line search is applied. In the EM framework, we can use any GLASSO solver available from the literature.

3.3 Debiasing the GLASSO

As stated earlier, the GLASSO uses an ℓ_1 regularization to promote sparsity. Although it achieves that goal, it also *penalizes the magnitude of nonzero entries* of \mathbf{Q} . We refer to this problem as the GLASSO bias. In fact, as we demonstrate later (see § 4), this bias is even more damaging in the mixture setting than in the single-Gaussian case. This is because of the following vicious cycle: the bias in the estimates of the \mathbf{Q}_k 's yields poor estimates of the w_{ki} weights during the E-step of the EM algorithm, and these, in turn, yield poorer estimates of the \mathbf{Q}_k 's in the M-step, and so forth. In fact, in § 4 we show the problem might be so severe that estimating a GMRF-MM using a naive application of GLASSO in the M step can yield such a poor estimate that one might be better off with the baseline GMM (*i.e.*, with no

Algorithm 2: Debiased Graphical LASSO**Input:** S, λ 1 $\hat{Q} \leftarrow \text{GLASSO}(S, \lambda)$ # Algorithm initialized by the GLASSO estimate from previous EM iteration.2 $Q \leftarrow$ The result of Algorithm 1 with $\Omega = \text{Supp}(\hat{Q})$ and $Q^{(0)} = \hat{Q}$ **Output:** Q

regularization or sparsity), despite the fact that the latter suffers from over-parameterization. To remove the bias effectively we suggest a two-step estimation procedure summarized in Algorithm 2. First, we use GLASSO (without penalizing the diagonal) and use its estimate of the sparsity pattern (but discard the GLASS estimates of the nonzero values) to define the graphical structure of each component of the mixture (different components can have different patterns). Then the second step is finding the MLE subject to that support, using the method described in § 3.1. More explicitly, suppose that \hat{Q}_k is estimated by GLASSO for component k . We then remove the ℓ_1 penalty and estimate Q_k such that $\text{Supp}(Q_k) \subseteq \text{Supp}(\hat{Q}_k)$. In summary, while this approach requires solving two optimization problems instead of one, it yields substantially better results, as we will show in § 4.

Remark 3 Instead of solving a single GLASSO problem, the underlying graphs of the precision matrices can also be estimated by solving n independent (non-Graphical) LASSO problems involving the data terms $\{x_i\}$ (Zhou et al., 2011). The estimated graphs can then be used as the support for the method described in § 3.1. Our experiments indicate that this approach yields comparable results to our approach, both in terms of the estimated graphs and the quality of the model. However, as the data in the EM is softly divided between components, the (rectangular) data matrix can be much larger than the empirical covariance in (5), and hence obtaining the pattern from the GLASSO estimate is cheaper in that case. Also, using the biased GLASSO estimates, we “warm start” each component’s precision-matrix estimation. This results in fewer iterations to convergence.

The choice of regularization parameter. Just like the standard GLASSO estimation requires a proper choice of λ , the debiased version also requires such a choice too. Obviously, the higher we choose λ the more sparse the estimated Q will be, *but it will also be more biased*. To truly promote sparsity, λ usually has to be substantial, which yields a substantially-biased estimation. Often, as we demonstrate later, the optimal choice of λ in GLASSO is essentially a compromise between promoting sparsity and reducing the bias effect in the estimation, leading to less sparsity in the estimation as one may be able to achieve without the bias. In our debiased GLASSO approach, we separate the sparsity promotion and the estimation of the nonzero values. Hence, the optimal value of λ for the sparsity estimation is larger than the one for the standard GLASSO alone, because then we are not required to reduce the bias effect.

Remark 4 The ℓ_1 regularization in GLASSO also plays the role of producing some tolerance to noise in the measurements. For this purpose, other simple regularization techniques such as Tikhonov or Riccati regularizations (Honorio and Jaakkola, 2013) (which do not promote sparsity) are also suitable. However, the amount of regularization needed for having tolerance to noise is usually lower than the regularization needed to promote sparsity; the latter often arises from different considerations, *e.g.*, reducing the number of parameters in the model. Once the sparsity is found, the debiased estimation can also be regularized for

the purpose of tolerance to noise in the measurements by ℓ_1 , Tikhonov, or any other suitable regularization approach. In any case, unless the noise level is very high, the noise-related regularization parameter will be much smaller than the one needed for promoting sparsity, leading to a proper noise-related bias in the estimation.

3.4 Theoretical results explaining the GLASSO bias

From a Bayesian perspective, the fact that GLASSO causes a bias is unsurprising: any Bayesian method (the ℓ_1 penalty can be interpreted in terms of a Laplace-distribution prior) pushes the estimate away from the MLE. Our point, however, is not that the bias exists but that it is substantial, arguably more than one might expect (regardless whether the diagonal is penalized or not). In this section we provide new theoretical results that shed some light upon this phenomenon.

First, we state a simple lemma, showing that if the inverse of the empirical covariance happens to be sparse with the same assumed support as that of the latent \mathbf{Q}_{TRUE} (the true unknown precision matrix), then it is the MLE of \mathbf{Q}_{TRUE} .

Lemma 1 *Suppose that \mathbf{S}^{-1} is sparse and that $\Omega = \text{Supp}(\mathbf{S}^{-1})$. Then \mathbf{S}^{-1} solves Eq. (10).*

Proof By the strict convexity of the problem (6), in addition to the (convex) linear constraints we have a unique solution to the sparsity-constrained problem. Since $\text{Supp}(\hat{\mathbf{Q}})$ trivially satisfies the optimality condition and the constraints, then it is the solution. \square

The following propositions show that when there is enough data such that \mathbf{S}^{-1} is sufficient to estimate the true latent \mathbf{Q}_{TRUE} with high accuracy (so $\hat{\mathbf{Q}}_{\text{MLE}} \approx \mathbf{Q}_{\text{TRUE}}$), the GLASSO estimate is still substantially far from \mathbf{Q}_{TRUE} , even if the sparsity pattern of the GLASSO estimate is correct.

Let the premise of Lemma 1 hold and let \mathbf{Q}_λ be the solution of Eq. (11), without penalizing the diagonal. Then, approximately, the off-diagonal entries of \mathbf{Q}_λ have opposite signs to those of the corresponding entries of \mathbf{S} . More precisely:

Proposition 1 *Let $\Omega = \text{Supp}(\mathbf{Q}_\lambda)$. Up to a first-order approximation we have that for all $(i, j) \in \Omega$ where $i \neq j$ we have*

$$|\mathbf{S}_{ij}| > \lambda \Rightarrow \text{sign}(\mathbf{S}_{ij}) = -\text{sign}((\mathbf{Q}_\lambda)_{ij}). \quad (17)$$

Proof The optimality condition of (11) states that if $(i, j) \in \Omega$

$$(\mathbf{Q}_\lambda^{-1})_{ij} = \begin{cases} \mathbf{S}_{ii} & i = j \\ \mathbf{S}_{ij} + \lambda \cdot \text{sign}((\mathbf{Q}_\lambda)_{ij}) & i \neq j \end{cases} \quad (18)$$

and otherwise

$$|(\mathbf{Q}_\lambda^{-1})_{ij} - \mathbf{S}_{ij}| < \lambda.$$

Let \mathbf{D}_Q be the diagonal matrix whose entries are the diagonal of \mathbf{Q}_λ . Then, according to the Neumann series we have

$$(\mathbf{D}_Q^{-1} \mathbf{Q}_\lambda)^{-1} = \mathbf{D}_Q \mathbf{Q}_\lambda^{-1} = \mathbf{I} - \tilde{\mathbf{Q}}_\lambda + \sum_{k=2}^{\infty} (-1)^k \tilde{\mathbf{Q}}_\lambda^k \quad (19)$$

where $\tilde{\mathbf{Q}}_\lambda$ is the off-diagonal part of the diagonally normalized matrix $\mathbf{D}_\mathbf{Q}^{-1}\mathbf{Q}_\lambda$. Since the diagonal of $\mathbf{D}_\mathbf{Q}$ is all positive, then using the first-order term of (19) on the right hand side of (18) yields for every $i \neq j$

$$(\mathbf{Q}_\lambda^{-1})_{ij} \approx (\mathbf{D}_\mathbf{Q}^{-1} - \mathbf{D}_\mathbf{Q}^{-1}\tilde{\mathbf{Q}}_\lambda)_{ij} = \mathbf{S}_{ij} + \lambda \cdot \text{sign}((\mathbf{Q}_\lambda)_{ij}), \quad (20)$$

which means that any off-diagonal entry (i, j) for which $|\mathbf{S}_{i,j}| > \lambda$ is non zero in \mathbf{Q}_λ ($(i, j) \in \text{Supp}(\mathbf{Q}_\lambda)$) up to the first-order approximation, and we have

$$(\mathbf{D}_\mathbf{Q})_{ii}^{-2}(\mathbf{Q}_\lambda)_{ij} = -\mathbf{S}_{ij} - \lambda \cdot \text{sign}((\mathbf{Q}_\lambda)_{ij}),$$

which proves the proposition for all off-diagonal entries (i, j) . \square

Suppose that the premise of Proposition 1 holds and assume that we have enough samples such that $\mathbf{S}^{-1} \approx \mathbf{Q}_{\text{TRUE}}$. Furthermore, assume that with a proper choice of λ , the support of the GLASSO minimizer \mathbf{Q}_λ is the true one. This will happen for example when \mathbf{Q}_{TRUE} is diagonally dominant, in which case the entries \mathbf{S}_{ij} decay rapidly with the graph distance between i and j on the graph associated with \mathbf{Q}_{TRUE} . This can be seen from the corresponding Neumann series in (19). The next proposition shows that even though it has the true support, the eigenvalues of \mathbf{Q}_λ can be substantially biased; *i.e.*, the GLASSO estimate, even without penalizing the diagonal, can be far from the MLE and the true solution.

Proposition 2 *Assume that \mathbf{Q}_λ has the true support; *i.e.*, $\text{Supp}(\mathbf{Q}_\lambda) = \text{Supp}(\mathbf{Q}_{\text{TRUE}})$. Let μ_i be the eigenvalues of \mathbf{Q}_λ^{-1} . Then, up to first-order approximation we have that*

$$|\mathbf{S}_{ii} - \mu_i| \leq \sum_{j \neq i: (i,j) \in \Omega} (|\mathbf{S}_{ij}| - \lambda) + \sum_{j \neq i: (i,j) \notin \Omega} (|\mathbf{S}_{ij} - \lambda \mathbf{E}_{ij}|) \quad (21)$$

where $|\mathbf{E}_{ij}| < 1$.

In words: even when GLASSO yields the true support, the eigenvalues of the GLASSO covariance matrix will likely be different from those of the empirical covariance \mathbf{S} even if that one approximates the true covariance $\mathbf{Q}_{\text{TRUE}}^{-1}$ well. Particularly, the Gershgorin radii are much smaller in comparison to those of \mathbf{S} as λ grows (while all conditions are satisfied), and the eigenvalues are much closer to the diagonal elements $\mathbf{S}_{i,i}$. Moreover, the smallest and largest eigenvalues are expected to be larger and smaller respectively as a result of the bias, indicating that estimated \mathbf{Q}_λ has an overly-optimistic condition number w.r.t. that of the true matrix. All this while at the same time the proposed sparsity-constrained MLE estimates \mathbf{Q}_{TRUE} well under the stated assumptions, and since the supports are identical, so does the debiased GLASSO estimate.

Proof From the optimality condition in Eq. (18) without penalizing the diagonal, we know that there exists a matrix \mathbf{E} such that

$$\mathbf{Q}_\lambda^{-1} = \mathbf{S} + \lambda \mathbf{E}, \quad (22)$$

where $\mathbf{E}_{ii} = 0$ for all i , and for $i \neq j$ we have that $\mathbf{E}_{ij} = \text{sign}((\mathbf{Q}_\lambda)_{ij})$ for $(i, j) \in \Omega$, and $|\mathbf{E}_{ij}| < 1$ otherwise. From the Gershgorin circle theorem we have that

$$|\mathbf{S}_{ii} - \mu_i| \leq \sum_{j \neq i} (|\mathbf{S}_{ij} - \lambda \mathbf{E}_{ij}|). \quad (23)$$

From Proposition 1 we have that up to a first order approximation, if an off-diagonal $(i, j) \in \text{Supp}(\mathbf{Q}_\lambda)$, and $|\mathbf{S}_{i,j}| > \lambda$ then $\mathbf{E}_{ij} = -\text{sign}(\mathbf{S}_{i,j})$. This, together with Eq. (23), concludes the proof. \square

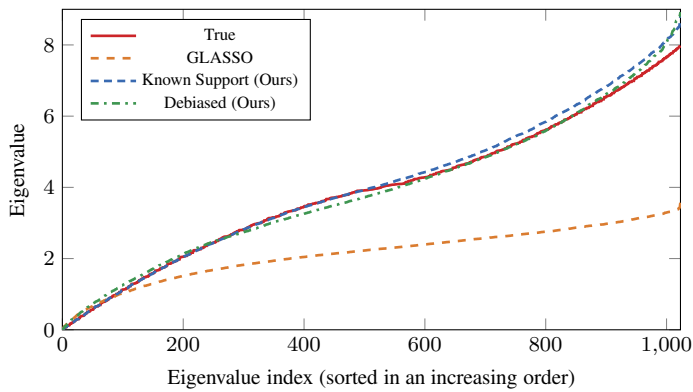


Fig. 1: A comparison of the eigenvalues of the real matrix and the three estimates. \mathbf{Q}_{TRUE} is induced by a 2D discrete Laplacian operator of the dimensions $32^2 \times 32^2$. The estimations were done using 300 samples. Known Support: our MLE estimator given the known support; GLASSO: The GLASSO estimator with $\lambda = 0.25$; Debiased: our MLE estimator with a support chosen to be the nonzero pattern as was estimated by the GLASSO.

We note that the results above will not be significantly different if we consider the original version of GLASSO where the diagonal is penalized.

4 Results

In this section, we validate the effectiveness of the proposed model and method via both synthetic- and real-data experiments in several settings. The first two synthetic-data experiments serve to present the GLASSO bias and how it is amplified in the mixture setting, and to demonstrate how the proposed method solves that problem effectively. The first set of real-data experiments are estimations of a single Gaussian for several gene-expression datasets. The second is learning GMMs over image patches, using the different approaches, and then use them as priors within a popular image-denoising method. Whenever we report a certain value of λ , either for the GLASSO method when used alone, or for the first step in our debiasing method, that value was empirically chosen to yield the best results for the respective method. All the experiments were done using a GLASSO implementation with no penalty on the diagonal elements.

4.1 The GLASSO bias

Our first experiment is the task of estimating the precision matrix of a single Gaussian. We drew 300 points, *i.i.d.*, from a zero-mean Gaussian in \mathbb{R}^{1024} whose precision matrix is induced by a homogenous discrete 2D Laplacian operator (for the connection between such a differential operator and a GMRF, see [Grenander and Miller \(2007\)](#)), whose stencil is given by

$$\begin{bmatrix} & -1 & \\ -1 & 4 & -1 \\ & -1 & \end{bmatrix}$$

for a 32-by-32 lattice. The data dimension, $n = 32^2 = 1024$, is larger than the number of samples, $N = 300$, making the empirical covariance matrix rank deficient.

We compare the eigenvalues of the real precision matrix with three of the estimates discussed earlier (in either the GLASSO method or the proposed debiased method, the GLASSO parameter, λ , is chosen according to the best empirical result for that method); see Fig. 1. It is evident from the figure that while both the proposed methods (known sparsity; debiased) obtain eigenvalues that are very close to the correct ones, the GLASSO tends to yield eigenvalues that are much smaller.

The observed differences show how significant the bias of the GLASSO can be, even in the single-Gaussian case, as well as the substantial improvement in estimation accuracy that is achieved by using the proposed debiasing method.

4.2 Synthetic data clustering

Our second experiment focuses on the task of clustering. To generate the synthetic data we draw 10 random sparse SPD matrices and use them as precision matrices of zero-mean Gaussian mixture components. Concretely, each matrix is defined by a finite-difference discretization of an anisotropic diffusion operator

$$\frac{\partial}{\partial x} \left(a(x, y) \frac{\partial}{\partial x} \right) + \frac{\partial}{\partial y} \left(b(x, y) \frac{\partial}{\partial y} \right)$$

on a regular 10×10 grid, where $a(x, y), b(x, y)$ are the positive diffusion coefficients, chosen at random uniformly. We then draw between 1,500 to 3,000 samples from each component to create a dataset. This way we generated 30 different datasets of random components.

For each dataset we use the EM-GMM algorithm described in § 2 to learn GMMs of several types, each is different only in the precision-matrix estimation procedure: 1) a baseline with no regularization (*i.e.*, $\mathbf{Q} = \mathbf{S}^{-1}$); 2) GLASSO estimator with $\lambda = 0.3$; 3) The proposed debiasing method with the same parameter; 4) The proposed method using the known support. Table 1 shows the mean and standard deviation of the Normalized Mutual Information (NMI) and Variation of Information (VI) achieved by the different configurations on the datasets.

Table 1: Synthetic-data Clustering

GMM type	NMI (higher is better)	VI (lower is better)
Baseline	0.61 ± 0.15	1.78 ± 0.67
GLASSO	0.03 ± 0.02	2.77 ± 0.18
Debiased (Ours)	0.92 ± 0.01	0.39 ± 0.12
Known Sparsity (Ours)	0.94 ± 0.02	0.29 ± 0.09

To summarize, the best score is of the proposed GMRF-MM using the known sparsity, showing this is the best choice when the graphical structure underlying the data is known. The GLASSO achieves a very poor result; in fact, it is even (far) worse than the baseline GMM, even though the latter is over-parameterized. In contrast, the proposed debiased method greatly outperforms the baseline, and achieves results that are almost equal to those obtained when we use the known sparsity.

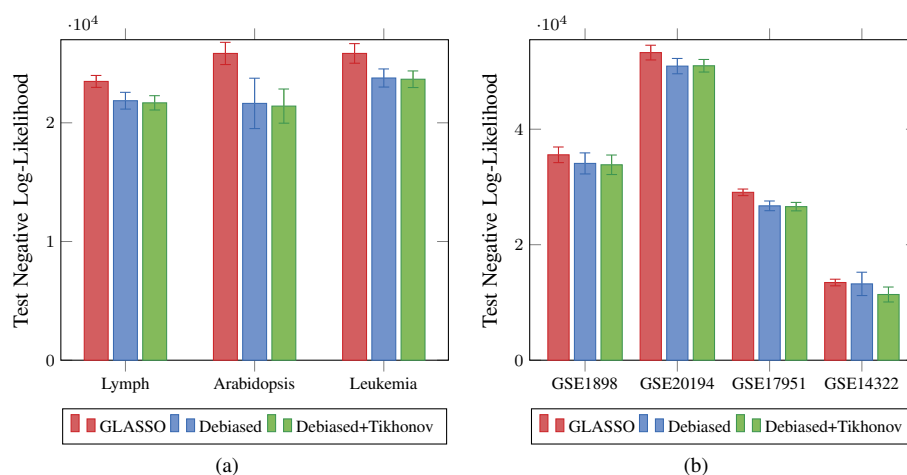


Fig. 2: Gene Expression mean negative log-likelihood (with standard deviation interval) for the test data. Lower is better. Comparing GLASSO with our Debiased and Debiased with Tikhonov regularization methods. (a) uses all the features of each dataset, while (b) uses 700 features chosen randomly for each test.

4.3 Gene expression data

The first real-world data we experiment with are gene-expression datasets reported in [Li and Toh \(2010\)](#); [Honorio and Jaakkola \(2013\)](#). In this application domain, estimating precision matrices is of interest as it facilitates the discovery of interactions between variables (gene expressions) in high-dimensional datasets. These datasets have many variables and very few samples, making the empirical covariance rank deficient. In this experiment, we compare GLASSO and our debiased method in estimating a single Gaussian for modeling each dataset.

Each dataset is preprocessed so each variable is of zero mean and unit variance. Then, we perform 30 repetitions, where in each repetition we randomly split the data to a train set (80%), and a test set (20%). Similarly to [Li and Toh \(2010\)](#); [Honorio and Jaakkola \(2013\)](#); [Treister et al. \(2016\)](#), the regularization parameter λ for GLASSO is chosen for each dataset to keep the number of nonzero entries in the precision matrix to be about 10 nonzeros per row and we compare the likelihood of the obtained model under this constraint. We use GLASSO, Debiased GLASSO, and Debiased GLASSO with a Tikhonov regularization with a small parameter. The latter is important since these are real data with a significant amount of noise (see Remark 4).

The first three datasets – Lymph, Arabidopsis, and Leukemia – have sample dimensions 587, 834, and 1255 respectively, and the number of samples in each is 147, 117, and 71. The results are presented in Fig. 2a. Because of the debiasing effect we can see 10%–20% improvement in the negative log-likelihood over that obtained by the GLASSO.

The next datasets we use are taken from the Gene Expression Omnibus¹. The dimensions of each sample are 20K–100K, and there are about 75–280 samples in each set. Similarly

¹ <https://www.ncbi.nlm.nih.gov/geo/>

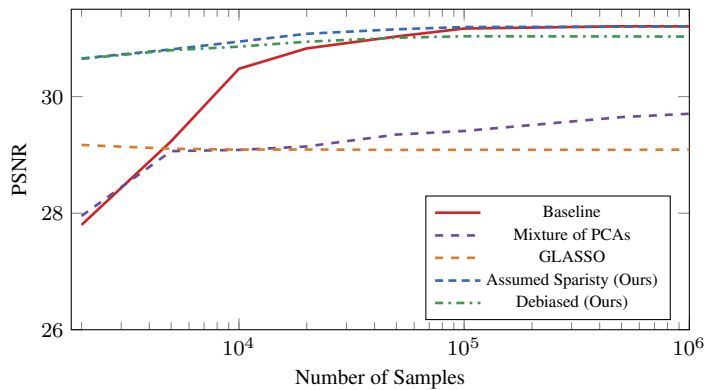


Fig. 3: Performance of the EPLL-based image restoration method with each of the estimated GMMs as prior, using varying numbers of training samples. The abscissa represents the number of samples used to train each model, and the ordinate represents the mean PSNR result (higher is better) for denoising 200 test images corrupted with a white Gaussian noise of $\sigma = 15$.

to [Honorio and Jaakkola \(2013\)](#), in each repetition, we randomly choose 700 features. The results are presented in Fig. 2b, and again show an advantage to the debiased estimates. We note that for this experiment since we choose only 700 features from each sample, we can choose quite low values of λ (and $\lambda \approx 0.5$). Having more features generally requires higher values of λ to yield sparsity of 10 nonzeros per row. Specifically, the full data requires values $\lambda \approx 0.7$ ([Treister et al., 2016](#)), further increasing the bias.

4.4 Image restoration with GMM prior

In the following experiments, we test the quality of our method for learning a prior for the task of image denoising. Particularly, we use an image-restoration method from [Zoran and Weiss \(2011\)](#) which is based on maximizing the Expected Patch Log-Likelihood (EPLL) while being close to the corrupted image. The restoration is achieved by minimizing the following objective function

$$f_p(\mathbf{x}|\mathbf{y}) = \frac{\alpha}{2}\|\mathbf{x} - \mathbf{y}\|^2 - \text{EPLL}_p(\mathbf{x}) \quad (24)$$

w.r.t. \mathbf{x} , where \mathbf{y} is the noisy image and $\alpha > 0$ is a balancing parameter. The EPLL is defined as

$$\text{EPLL}_p(\mathbf{x}) = \sum_i \log p(\mathbf{P}_i \mathbf{x}) \quad (25)$$

where \mathbf{P}_i is a projection matrix that extracts the i -th patch from the image. The prior p proposed by [Zoran and Weiss \(2011\)](#) is a GMM learned over the pixels of natural image patches. In this experiment we use it as a “black box” and change only the GMM priors. We use the Peak Signal-to-Noise Ratio (PSNR) between the clean images and the reconstructions as a means to measure the quality of each GMM type in modeling natural image patches.

For this, we have implemented a version of the EPLL method in Python, which was adapted from the Matlab code of [Zoran and Weiss \(2011\)](#), which was written for grayscale

images, to also work with RGB images. We set the restoration method to run 5 iterations for each image. Each experiment specifies the GMMs learning configurations. All of the learning tasks were done using randomly-selected patches taken from the Berkeley Segmentation Dataset (Martin et al., 2001) (BSD) training set, and all tests were done on the BSD test set.

4.4.1 Grayscale images

The first experiment in this set is for grayscale images. Treating the $d \times d$ patch as a graph with $n = d^2$ vertices, we define a neighborhood system that connects all vertices in an $m \times m$ region. As explained in § 2, this creates a sparsity pattern for each component’s precision matrix. Enforcing such sparsity reduces the number of nonzero parameters from $O(d^4)$ to $O(d^2 m^2)$.

For this experiment we set K , the number of Gaussians, to 100, and change only the size of the training set each time. The parameter λ was picked according to the best empirical result for the smallest training set, and kept while increasing the set size. We use our EM-GMM implementation to learn several GMMs, each is different only in the precision matrix estimation process: 1) A baseline GMM with no regularization (*i.e.*, $\mathbf{Q} = \mathbf{S}^{-1}$); 2) A mixture of 30-dimensional PCA subspaces (Tipping and Bishop, 1999); 3) The GLASSO estimator with $\lambda = 0.7$; 4) The proposed debiased method with the same parameter; 5) The proposed method using the sparsity pattern described above with $m = 5$.

To test the quality of each of the GMMs we use the denoising algorithm described above to denoise the 200 images of the BSD test set corrupted with a white Gaussian noise of $\sigma = 15$. Figure 3 shows the mean PSNR result of each GMM type as a function of the size of the training set. The figures show that the smaller the training set is, the worse the results of the baseline GMM are, and that the proposed method using the assumed sparsity clearly outperforms it. As the number of samples grows, the baseline GMM and our GMRF-MM achieve comparable performance, *even though our approach has far fewer parameters*. Also, we see that the proposed debiasing method achieves better results than GLASSO. This shows that when we cannot assume the graphical structure of the data, our debiasing method is still preferable over GLASSO. Results for other noise levels (values of σ) showed a similar trend.

4.4.2 Color images

The next experiment we present is for RGB images, where each pixel has 3 color channels. In this scenario, each patch is of size $d \times d \times 3$. We define a neighborhood system such that each pixel is connected to the $m \times m$ pixels over all of the color channels. We set K to 200, and learn the four models using 10^6 RGB patches taken randomly from the BSD training set. We learn two types of GMMs, one with an assumed sparsity using $m = 5$, and a baseline GMM with no regularization. Each image from the BSD test set is first corrupted using a random σ in the range of 10 to 100 and is then denoised with each of the learned priors. Earlier, with grayscale images, we saw that 10^5 samples were about enough for the baseline GMM to achieve similar results to the proposed GMRF-MM. Here, when the dimensionality is higher we show that the proposed model is more effective than the baseline even when their common training set is larger: Figure 4 shows the performance gain from using the proposed method. Every point above the line represents an image, corrupted with random noise, on which a better PSNR result was obtained when denoised with our GMRF-MM. The gain is fairly consistent, even though our model uses far fewer parameters.

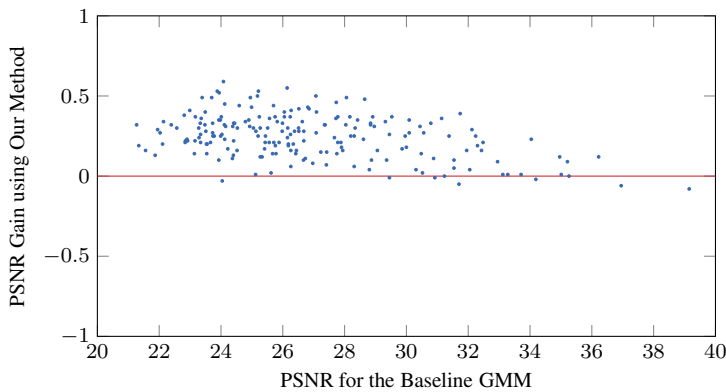


Fig. 4: Comparison of the performance of RGB image denoising using the EPLL [Zoran and Weiss \(2011\)](#), extended from grayscale to color images. The two priors are a baseline GMM, and a GMRF-MM with an assumed sparsity. Both priors are learned using 10^6 patches of size $8 \times 8 \times 3$, with $K = 200$. Each image was corrupted with a white gaussian noise of random σ .

5 Conclusion

In this work, we proposed a GMRF mixture model to mitigate the over-parameterization effect that classical GMMs are prone to in the presence of data scarcity. We presented an effective way to learn such a model in two cases: one is when the sparsity pattern of the precision matrices is assumed, and the other is when that pattern needs to be estimated. The latter is the more complicated scenario, for which we showed that a naive approach of incorporating the GLASSO estimator in the traditional GMM framework leads to unfavorable models due to a biasing effect of the ℓ_1 regularizer in GLASSO. To overcome this, we proposed a two-stage estimation procedure where in the first stage only the sparsity pattern is estimated via GLASSO, while in the second stage the sparsity is held fixed, the ℓ_1 regularization is reduced, and a Newton-type optimization method is used to find the globally-optimal precision matrix. We showed in our numerical results that in many scenarios the baseline standard GMM can produce unfavorable models, and restricting its parameters can improve the estimated models. We also showed that the model produced by GLASSO is consistently improved by the debiasing stage, and in several cases can outperform the standard GMM - especially when the data is insufficient for effective learning of the latter.

We reiterate that our main motivation is related to the mixture-model case, where both the over-parameterization and the LASSO bias are far more drastic (than they are with a single Gaussian); this case was not well studied before. Thus, the success of the novel proposed method in the single-Gaussian case should not detract the reader from appreciating its more important success in the mixture-model setting.

Our framework can be especially effective in scenarios where the dimensions are high, the underlying distribution has a large number of modes, and the data is scarce w.r.t. the number of parameters associated with the multimodal distribution. Another interesting utility of our method, which we did not explore here, is to exploit the sparsity and compactness of the learned GMRF-MM to gain computational benefits during inference tasks where that model is used. For example, the EPLL framework for image restoration might be able to lever-

age computational tools from sparse linear algebra to speed up computations and reduce its memory footprint.

References

- Azizyan M, Singh A, Wasserman L (2015) Efficient sparse clustering of high-dimensional non-spherical gaussian mixtures. In: *Artificial Intelligence and Statistics*, pp 37–45 [2](#)
- Basharat A, Gritai A, Shah M (2008) Learning object motion patterns for anomaly detection and improved object detection. In: *2008 IEEE Conference on Computer Vision and Pattern Recognition, IEEE*, pp 1–8 [2](#)
- Bollhöfer M, Eftekhari A, Scheidegger S, Schenk O (2019) Large-scale sparse inverse covariance matrix estimation. *SIAM Journal on Scientific Computing* 41(1):A380–A401 [2](#)
- Bouveyron C, Girard S, Schmid C (2007) High-dimensional data clustering. *Computational Statistics & Data Analysis* 52(1):502–519 [2](#)
- Chen X, Yang J, Zhang J, Waibel A (2004) Automatic detection and recognition of signs from natural scenes. *IEEE Transactions on image processing* 13(1):87–99 [2](#)
- Freifeld O, Li Y, Fisher JW (2015) A fast method for inferring high-quality simply-connected superpixels. In: *ICIP, IEEE* [2](#)
- Friedman J, Hastie T, Tibshirani R (2008) Sparse inverse covariance estimation with the graphical lasso. *Biostatistics* 9(3):432–441 [2](#), [5](#)
- Friedman J, Hastie T, Tibshirani R (2010) Regularization paths for generalized linear models via coordinate descent. *Journal of statistical software* 33(1):1 [7](#)
- Grenander U, Miller M (2007) *Pattern theory: from representation to inference*. Oxford University Press, USA [2](#), [11](#)
- Hastie T, Tibshirani R, Friedman J, Franklin J (2005) The elements of statistical learning: data mining, inference and prediction. *The Mathematical Intelligencer* 27(2):83–85 [1](#)
- Honorio J, Jaakkola TS (2013) Inverse covariance estimation for high-dimensional data in linear time and space: Spectral methods for riccati and sparse models. *arXiv preprint arXiv:13096838* [8](#), [13](#), [14](#)
- Hsieh CJ, Sustik MA, Dhillon IS, Ravikumar PK, Poldrack R (2013) Big & quic: Sparse inverse covariance estimation for a million variables. In: *Advances in neural information processing systems*, pp 3165–3173 [2](#)
- Hsieh CJ, Sustik MA, Dhillon IS, Ravikumar P (2014) Quic: quadratic approximation for sparse inverse covariance estimation. *The Journal of Machine Learning Research* 15(1):2911–2947 [2](#), [6](#), [7](#)
- Idé T, Khandelwal A, Kalagnanam J (2016) Sparse gaussian markov random field mixtures for anomaly detection. In: *2016 IEEE 16th International Conference on Data Mining (ICDM), IEEE*, pp 955–960 [2](#)
- Jelisavcic V, Stojkovic I, Milutinovic V, Obradovic Z (2018) Fast learning of scale-free networks based on cholesky factorization. *International Journal of Intelligent Systems* 33(6):1322–1339 [2](#)
- Jepson A, Black MJ (1993) Mixture models for optical flow computation. In: *Proceedings of IEEE Conference on Computer Vision and Pattern Recognition, IEEE*, pp 760–761 [2](#)
- Kawabata T (2008) Multiple subunit fitting into a low-resolution density map of a macromolecular complex using a gaussian mixture model. *Biophysical journal* 95(10):4643–4658 [2](#)

- Khare K, Oh SY, Rahman S, Rajaratnam B (2019) A scalable sparse cholesky based approach for learning high-dimensional covariance matrices in ordered data. *Machine Learning* 108(12):2061–2086 [2](#)
- Koller D, Friedman N (2009) Probabilistic graphical models: principles and techniques. MIT press [2](#)
- Krishnamurthy A (2011) High-dimensional clustering with sparse gaussian mixture models. Unpublished paper pp 191–192 [2](#)
- Li L, Toh KC (2010) An inexact interior point method for l_1 -regularized sparse covariance selection. *Mathematical Programming Computation* 2(3-4):291–315 [13](#)
- Li SZ (1994) Markov random field models in computer vision. In: European conference on computer vision, Springer, pp 361–370 [3](#)
- Lotsi A, Wit E (2016) Sparse gaussian graphical mixture model. *Afrika Statistika* 11(2):1041–1059 [2](#)
- Martin D, Fowlkes C, Tal D, Malik J, et al. (2001) A database of human segmented natural images and its application to evaluating segmentation algorithms and measuring ecological statistics. *Iccv Vancouver*: [15](#)
- McLachlan GJ, Lee SX, Rathnayake SI (2019) Finite mixture models. *Annual review of statistics and its application* 6:355–378 [2, 4](#)
- Nagoshi E, Saini C, Bauer C, Laroche T, Naef F, Schibler U (2004) Circadian gene expression in individual fibroblasts: cell-autonomous and self-sustained oscillators pass time to daughter cells. *Cell* 119(5):693–705 [2](#)
- Niknejad M, Bioucas-Dias J, Figueiredo MA (2019) External patch-based image restoration using importance sampling. *IEEE Transactions on Image Processing* 28(9):4460–4470 [2](#)
- Oh S, Dalal O, Khare K, Rajaratnam B (2014) Optimization methods for sparse pseudolikelihood graphical model selection. In: *Advances in Neural Information Processing Systems*, pp 667–675 [2](#)
- Papayan V, Elad M (2015) Multi-scale patch-based image restoration. *IEEE Transactions on image processing* 25(1):249–261 [2](#)
- Pyun K, Lim J, Won CS, Gray RM (2007) Image segmentation using hidden markov gaussian mixture models. *IEEE Transactions on Image Processing* 16(7):1902–1911 [2](#)
- Reynolds DA, Rose RC (1995) Robust text-independent speaker identification using gaussian mixture speaker models. *IEEE transactions on speech and audio processing* 3(1):72–83 [2](#)
- Reynolds DA, Quatieri TF, Dunn RB (2000) Speaker verification using adapted gaussian mixture models. *Digital signal processing* 10(1-3):19–41 [2](#)
- Roth S, Black MJ (2005) Fields of experts: A framework for learning image priors. In: *2005 IEEE Computer Society Conference on Computer Vision and Pattern Recognition (CVPR'05)*, Citeseer, vol 2, pp 860–867 [3](#)
- Rue H, Held L (2005) Gaussian Markov random fields: theory and applications. Chapman and Hall/CRC [2, 5](#)
- Saad Y (2003) Iterative methods for sparse linear systems, vol 82. *siam* [6](#)
- Silvey SD (1970) Statistical inference. Routledge [4](#)
- Song HR, Fuentes M, Ghosh S (2008) A comparative study of gaussian geostatistical models and gaussian markov random field models. *Journal of Multivariate analysis* 99(8):1681–1697 [3](#)
- Stauffer C, Grimson WEL (1999) Adaptive background mixture models for real-time tracking. In: *Proceedings. 1999 IEEE Computer Society Conference on Computer Vision and Pattern Recognition (Cat. No PR00149)*, IEEE, vol 2, pp 246–252 [2](#)

- Tavassolipour M, Karamzade A, Mirzaeifard R, Motahari SA, Shalmani MTM (2019) Structure learning of sparse ggms over multiple access networks. *IEEE Transactions on Communications* 2
- Tipping ME, Bishop CM (1999) Mixtures of probabilistic principal component analyzers. *Neural computation* 11(2):443–482 15
- Treister E, Turek JS (2014) A block-coordinate descent approach for large-scale sparse inverse covariance estimation. In: *Advances in neural information processing systems*, pp 927–935 6, 7
- Treister E, Yavneh I (2012) A multilevel iterated-shrinkage approach to l_1 penalized least-squares minimization. *IEEE Transactions on Signal Processing* 60(12):6319–6329 7
- Treister E, Turek JS, Yavneh I (2016) A multilevel framework for sparse optimization with application to inverse covariance estimation and logistic regression. *SIAM Journal on Scientific Computing* 38(5):S566–S592 2, 13, 14
- Uziel, et al. (2019) Bayesian adaptive superpixel segmentation. In: *ICCV* 2
- Vandenberghe L, Andersen MS (2015) Chordal graphs and semidefinite optimization. *Foundations and Trends® in Optimization* 1(4):241–433 6
- Vila JP, Schniter P (2013) Expectation-maximization gaussian-mixture approximate message passing. *IEEE Transactions on Signal Processing* 61(19):4658–4672 2
- Vo BN, Ma WK (2006) The gaussian mixture probability hypothesis density filter. *IEEE Transactions on signal processing* 54(11):4091–4104 2
- Wainwright MJ (2019) *High-dimensional statistics: A non-asymptotic viewpoint*, vol 48. Cambridge University Press 2, 5
- Wang C, Jiang B (2020) An efficient admm algorithm for high dimensional precision matrix estimation via penalized quadratic loss. *Computational Statistics & Data Analysis* 142:106812 2
- Yang J, Liao X, Chen M, Carin L (2014) Compressive sensing of signals from a gmm with sparse precision matrices. In: *Advances in Neural Information Processing Systems*, pp 3194–3202 2
- Zhang RY, Fattahi S, Sojoudi S (2018) Large-scale sparse inverse covariance estimation via thresholding and max-det matrix completion. In: *International Conference on Machine Learning* 6
- Zhou S, Rütimann P, Xu M, Bühlmann P (2011) High-dimensional covariance estimation based on gaussian graphical models. *Journal of Machine Learning Research* 12(Oct):2975–3026 8
- Zhuang X, Huang Y, Palaniappan K, Zhao Y (1996) Gaussian mixture density modeling, decomposition, and applications. *IEEE Transactions on Image Processing* 5(9):1293–1302 2
- Zibulevsky M, Elad M (2010) $L1$ - $L2$ optimization in signal and image processing. *IEEE Signal Processing Magazine* 27(3):76–88 7
- Zoran D, Weiss Y (2011) From learning models of natural image patches to whole image restoration. In: *2011 International Conference on Computer Vision, IEEE*, pp 479–486 2, 14, 16